

Titanium Phosphinimide Polymerization Catalysts

Motivation

We are all familiar with the importance of Ziegler-Natta catalysis [TiCl_4 and co-catalyst Et_3Al], and the polymerisation of olefins which represents an important industrial process. The Ziegler-Natta catalyst is a solid state species, stereospecificity is controlled and the temperature and pressure under which the reaction occurs lowered. Zirconocene derivatives particularly Cp_2ZrR_2 are related single site catalysts, active without the need for a co-catalyst. A great deal of work has been carried out investigating these group IV metal compounds both synthetically and computationally and a huge array of ligands and centers have been examined for catalytic activity. The two papers under consideration examine the possibility of using zirconium and titanium phosphinimide complexes as possible single site catalysts. Other key catalysts in this area include those with bulky diamide ligands and metallocene based constrained geometry catalysts.

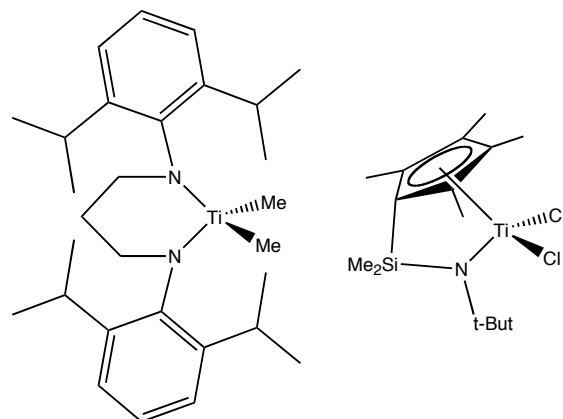


Figure 1 Examples of catalyst precursors

Phosphinimides have been investigated recently and have exhibited some catalytic ability. Small phosphinimide ligands lead to deactivation, but bulky ligands have been shown to sustain high activity under industrial type conditions. In this paper the catalytic cycle for a series of model compounds is studied.

The electron donating ability of the phosphinimide is altered by electron donating or withdrawing substituents. A series of bulky phosphinimide ligands has then been synthesised and their catalytic ability investigated.

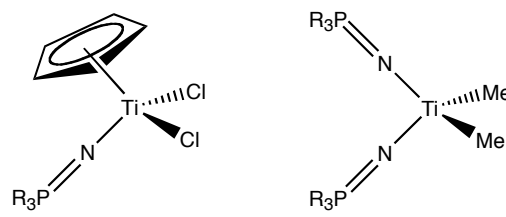


Figure 2 Phosphinimide Compounds

Reference

C. Beddie, E. Hollink, P. Wei, J. Gault, and D. Stephan, *Organometallics*, 2004, 23, 5240

Computational Details

- Not discussing force field methods
- Specified programs used: Gaussian and which release. This is so someone can reproduce the results *exactly* should they want to try.
- DFT => which functional?
 - Becke3 exchange
 - LYP correlation
 - =>B3LYP
- Optimised geometries using "LanL2DZ" but also looked for better energies by doing single point calculations at these geometries using a better basis set, BS2
- The Gaussian manual indicates that LanL2DZ places D95V on first row, and Los Alamos ECP plus DZ on Na-Bi. Then says D95V= Dunning/Huzinaga valence double-zeta, and LanL2 =Hay & Wadt ECP.
- Thus, the first row atoms all have all-electron basis sets, PP only start at Na, this means P, Cl and metals, eg
 - Ti=1s²2s²2p⁶3s²3p⁶3d⁴
 - ECP has replaced 1s²2s²2p⁶
 - Cl=1s²2s²2p⁶3s²3p⁵
 - ECP has replaced 1s²2s²2p⁶
- BS2 6-31G(d,p) on H, B, C, N, F (remember (d,p) means polarisation functions, a set of d functions for not-H atoms, and a set of p functions for the H atoms)
- BS2 has used the Gaussian implemented standard basis sets for Ti, Ni, P and Cl. But has supplemented the Ti basis set by a set of p functions, details determined by Couty and Hall, and a reference is supplied. And has added extra diffuse d function to P, and has explicitly given the exponent and referenced the source.
- COSMO is a method, implemented in Gaussian, for modelling the solvent as a polarizable continuum, ie not as individual molecules but as a responsive field. It is the most primitive way of including solvent effects.
- The characterisation of the reaction path is discussed, that is, the structures are identified by frequency analysis. The "real" reaction coordinates were not located, but a good guess is that they relate to the M-CH₃ and ethylene bonds so these were used to establish a path connecting reactants, TS and products.
- Mulliken analysis is a type of population analysis, we will be discussing these next week.

Computational Chemistry.

Molecular mechanics calculations were conducted using the MM3 force field as implemented in CAChe 6.0 for windows developed by CACHE Group, Fujitsu. All DFT calculations were performed using the Gaussian 98 suite of programs.⁸³ Optimized gas phase geometries were obtained using the Becke3 exchange functional,⁸⁴ as implemented in Gaussian^{98,85} in combination with the Lee, Yang, and Parr correlation functional,⁸⁶ i.e., the B3LYP method. The LANL2DZ basis set was used for geometry optimizations and energy calculations. Relative energies were obtained by performing single-point calculations at the B3LYP/

BS2 level of theory, based on the above geometries. The BS2 basis set is a larger basis set consisting of the 6-31G(d,p) basis set⁸⁷⁻⁹⁰ for H, B, C, N, and F atoms, and the LANL2DZ basis sets for Ti, Ni, P, and Cl. As previously recommended by Torrent, Sola⁹¹, and Frenking,⁹¹ for Ti, the LANL2DZ basis set was supplemented with a set of (n)p functions for transition metals developed by Couty and Hall.⁹² In addition, for P, a d function with an exponent of 0.34 was added.⁹³ This basis set is expected to provide more reliable relative energies than the smaller LANL2DZ basis set. Solvent effects were approximated

with single-point calculations using B3LYP/BS2 on gas phase B3LYP/LANL2DZ geometries using the COSMO method⁹⁴ with the dielectric constant of 2.379 for toluene. Toluene was chosen since all polymerization experiments reported herein used toluene as the solvent. The nature of transition structures was confirmed by calculating the harmonic vibrational frequencies. Relaxed potential energy scans along the C-C bond distances that served as the reaction coordinates, followed by full geometry optimizations, were used to confirm that all transition states were connected backward to the reactants and forward to the products. Atomic charges on titanium reported herein are Mulliken charges from the B3LYP/BS2 COSMO single-point calculations (Table 3). All relative energies are reported in kcal mol⁻¹, bond lengths in angstroms (Å), and angles in degrees (°), unless otherwise noted.

with single-point calculations using B3LYP/BS2 on gas phase B3LYP/LANL2DZ geometries using the COSMO method⁹⁴ with the dielectric constant of 2.379 for toluene. Toluene was chosen since all polymerization experiments reported herein used toluene as the solvent. The nature of transition structures was confirmed by calculating the harmonic vibrational

frequencies. Relaxed potential energy scans along the C-C bond distances that served as the reaction coordinates, followed by full geometry optimizations, were used to confirm that all transition states were connected backward to the reactants and forward to the products. Atomic charges on titanium reported herein are Mulliken charges from the B3LYP/BS2 COSMO single-point calculations (Table 3). All relative energies are reported in kcal mol⁻¹, bond lengths in angstroms (Å), and angles in degrees (°), unless otherwise noted.

The mechanism for ethylene polymerisation

The paper follows the polymerisation process for the addition of two ethylene molecules, however, here we will study in detail only the first process, **Figure 3**.

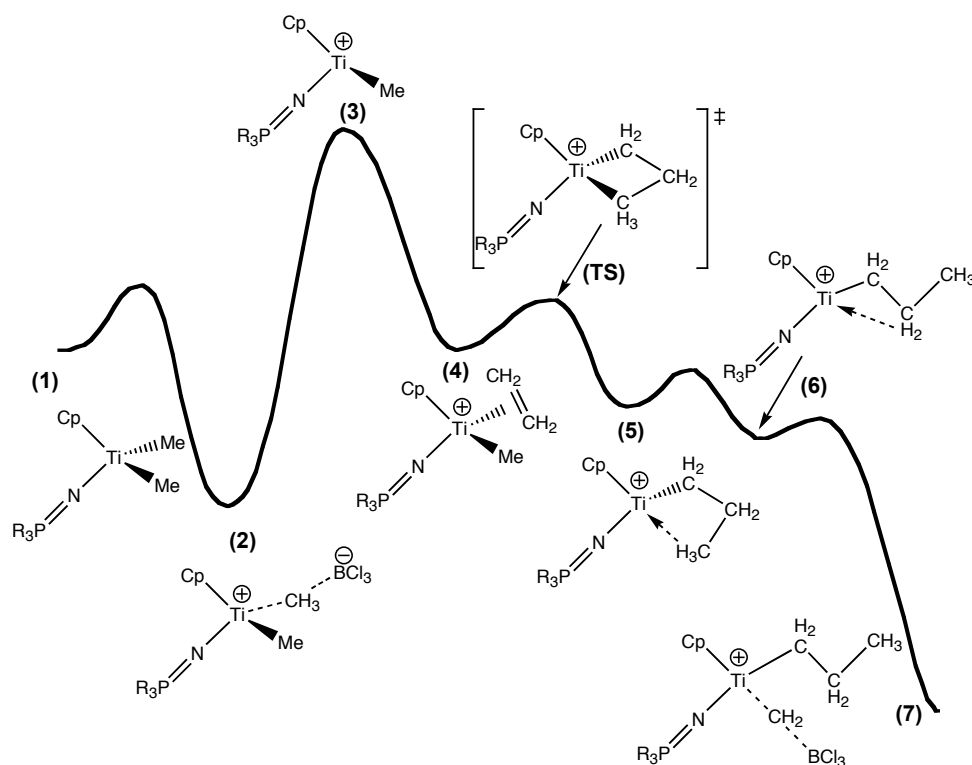


Figure 3 Energy profile and reaction mechanism for ethylene polymerisation

The polymerisation mechanism has been studied using the model compound $\text{CpTiMe}_2(\text{NPH}_3)$ (**1**) and the Lewis base BCl_3 , Figure 3 shows an approximate energy diagram for the reaction. The first process is the formation of an ion pair $[\text{CpTiMe}(\text{NPH}_3)]^+[\text{MeBCl}_3]^-$ (**2**), and then separation of the ion pair, $[\text{CpTiMe}(\text{NPH}_3)]^+$ (**3**). Addition of the ethylene to (**3**) forms (**4**) which inserts into the Ti- CH_3 bond via a cyclic transition state (**TS**) and forms (**5**), a propyl cation which exhibits a γ -agostic interaction the Ti center. The barrier for rearrangement to the β -agostic isomer (**6**) is only 5.9 kcal/mol. Re-coordination of the $[\text{MeBCl}_3]^-$ counter ion forms the stable ion pair $[\text{CpTiPr}(\text{NPH}_3)]^+[\text{MeBCl}_3]^-$ (**7**).

Here the geometry of each reactant, intermediate, and product has been located via minimisation. Each of these structures has been confirmed as a local minima by frequency analysis. This is *essential*, otherwise we don't know that a minimum has been located. The search algorithms for finding minima can look "finished" but then you will find a negative frequency indicating the minimization has not completed. Once a minimum has been located the energy is evaluated at a higher level using BS2.

This energy-path diagram provides a great deal of information about the reaction mechanism. It will tell us the rate determining step, ie the step with the largest barrier to overcome. It will show us how the reaction proceeds, by identifying the geometrical changes that take one structure to another. It will show us what the transition states look like, allowing us to make predictions about how to stabilise (enhance the reaction) or destabilise (inhibit side reactions) a particular mechanism. This diagram can tell us if there is one large energy barrier to overcome, or a number

of smaller ones. The details of this mechanism have been re-enforced by experimental evidence on similar compounds and back up the structures and energies proposed.

Note that in the paper there are several sections where the "potential energy" line is broken up, this indicates that the reaction path has not been followed over this region, or that transition states could not be found that linked the two minima together. This is not entirely satisfactory, but is a rather common problem. For example the TS between the γ -agostic structure (5) and the β -agostic structure (6) has not been located. Note also that only one transition state has specifically been identified, and that is the olefin insertion TS. Transition states are identified by one, *and only one*, imaginary frequency. The imaginary frequency will tell us what motion (or coordinates) link the two minima.

Structure (3) is not clearly identified as a "TS" because from the text it is clear the ion pair has been minimised and then the positive ion $[\text{CpTiMe}(\text{NPH}_3)]^\oplus$ has been minimised on its own to give the "energy jump" that is seen on the diagram.

Solvent Effects

Not shown on the diagram reproduced above are solvent effects. The continuum solvent model used in these calculations can only have an "average" effect the structures under study, no specific or local solute-solvent interactions can occur. The primary effect of this solvent model is to give slightly better geometries and energies compared to the gas phase. However, it is clear that even a "general" solvent environment significantly lowers the overall energy of the reaction, **Table 1**. This is of particular importance when charged species are reacting, as in this reaction mechanism. The solvent is providing a polar environment and can significantly stabilise individual ions. This effect can be seen in the column headed $\Delta(3-2)$. The relative energy of neutral species remains reasonably accurate in the gas phase, for example compare the data in columns headed $\Delta(3-4)$, $\Delta(\text{TS-4})$, and $\Delta(\text{TS-5})$.

H	1	2	$\Delta(3-2)$	3	$\Delta(3-4)$	4	$\Delta(\text{TS-4})$	TS	$\Delta(\text{TS-5})$	5	6	7
toluene	0	-19.1	35.5	25.4	18.9	6.5	6.0	12.5	15.4	-2.9	-5.8	-37.2
gas phase	0	-14.3	89.1	74.8	21.4	53.4	6.8	60.2	15.3	44.9	41.8	-34.4

Table 1 Solvent vs gas phase energies

Ligand Effects

Ligand effects have been studied by examining the stability of model compounds with different substituents on the NPR_3 ligand, for the olefin polymerisation reaction. The substituents range from electron donating substituents, CH_3 and NH_2 through H to electron withdrawing substituents, Cl and F. Details can be found in the paper, here we will examine the most electron donating substituent Me (ie $[\text{CpTiMe}(\text{NPMe}_3)]^+$) and the most electron withdrawing substituent F (ie $[\text{CpTiMe}(\text{NPF}_3)]^+$). The effect of these substituents on the complex energies are given in **Table 2**. The energy profile of the earlier figure was for the H substituent, in **Figure 4** data and a rough energy profile are given for Me vs F substituents.

R	1	2	3	4	TS1	5	6	7
Me	0	-23.7	17.3	0	6.4	-9.1	-12.8	-42.2
H	0	-19.1	25.4	6.5	12.5	-2.9	-5.8	-37.2
F	0	-5.6	40.5	19.8	24.5	9.6	7.4	-27.2

Table 2 Calculated solution phase relative energies in (kcal/mol)

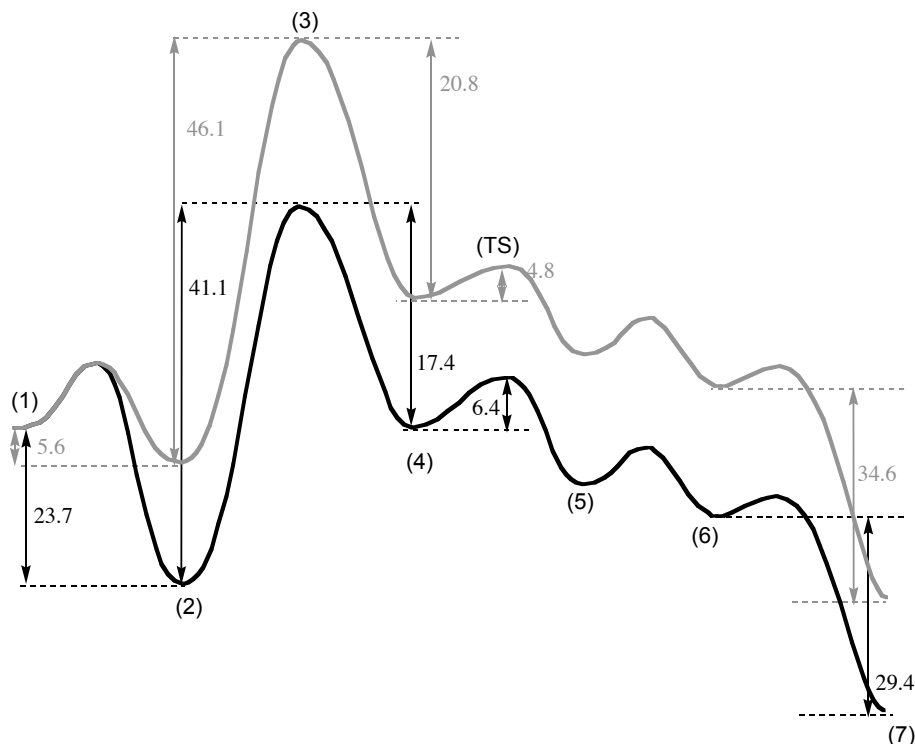


Figure 4 Effect of substituents on the reaction mechanism.

Electron withdrawing substituents destabilise the formation of the ion-pair significantly (stability of 2 has decreased ≈ 18 kcal/mol). However it is slightly harder to separate the ion-pair into the isolated charged species (since it takes 46.1 (F) vs 41.1 (Me) kcal/mol to form 3). The electron withdrawing group however favours the addition of ethylene (stabilisation of 20.8 (F) vs 17.4 (Me) kcal/mol), and has a lower barrier to migratory insertion (4.8 (F) vs 6.4 (Me) kcal/mol). The ion-pair product (7) is also more stable than the isolated ion (6) (34.6 (F) vs 29.4 (Me) kcal/mol). However, these effects do not compensate for the very important fact that the product, $[\text{CpTiPr}(\text{NPF}_3)][\text{MeBCl}_3]$ is substantially higher in energy than the product $[\text{CpTiPr}(\text{NPM}_e_3)][\text{MeBCl}_3]$ (-27.2 (F) vs -42.2 (Me) kcal/mol).

It was noted in the paper that there was some difficulty in determining the stability of the final product, ie reintroducing the counter ion to the β -agostic complex for the Cl and F compounds. In this case side reactions occurred. The authors tried to force the geometry to obtain a structure that is perhaps energetically possible, but unlikely to form.

A key result is that ion pair formation and dissolution have a very important role to play in olefin polymerisation, and in this case where the coordinating ligands are small, a more important role than the barrier height to ethylene migration and insertion. The ion pair separation energies are strongly effected by the electronic properties of the phosphinimide ligand, electron donating substituents stabilise this process (by ≈ 18 kcal/mol). The same substituents will effect the barrier to ethylene

complexation and insertion but by a much smaller amount (≈ 3 kcal/mol), electron donating substituents *increase* the barrier.

The conclusion drawn is that amino and alkyl substituents should be used to facilitate ion separation, from which follows ethylene coordination and thus polymerisation. A factor not able to be recovered in the calculations is the fact that only ligands which are sterically demanding lead to high polymerisation activity. The paper goes on to discuss the synthetic routes to a number of possible catalyst precursors. Those examined include $[\text{CpTiCl}_2(\text{NPR}_2)_3]$, $[\text{Cp}^*\text{TiCl}_2(\text{NPR}_2)_3]$, $[\text{CpTiMe}_2(\text{NPR}_2)_3]$, and $[\text{Cp}^*\text{TiMe}_2(\text{NPR}_2)_3]$ where R= Me, Et, Pr, Bu, i-PrMe, and EtPh. The best catalyst of those tested was $[\text{Cp}^*\text{TiMe}_2(\text{NPR}_2)_3]$ with R=Pr which had an activity of 10000 $\text{gmmol}^{-1}\text{h}^{-1}\text{atm}^{-1}$ compared to $[\text{Cp}_2\text{ZrMe}_2]$ which has an activity of 16000.